

External Grant Award Nos. 08HQGR0064 and 08HQGR0066

**VALIDATION OF 3D VELOCITY STRUCTURE IN THE SAN FRANCISCO BAY AREA
PHASE II: COLLABORATIVE RESEARCH WITH THE UNIVERSITY OF
CALIFORNIA, BERKELEY, AND THE UNIVERSITY OF MINNESOTA, DULUTH**

Douglas Dreger
Seismological Laboratory, University of California, Berkeley
215 McCone Hall #4760
Berkeley, CA 94720
Telephone: (510) 643-1719
FAX: (510) 643-5811
Email: dreger@seismo.berkeley.edu

David Dolenc
Large Lakes Observatory, University of Minnesota, Duluth
2205 E 5th Street
Duluth, MN 55812
Telephone: (218) 726-8136
FAX: (218) 726-6979
Email: ddolenc@d.umn.edu

Start Date: March 1, 2008
End Date: February 28, 2009

External Grant Award Nos. 08HQGR0064 and 08HQGR0066

**VALIDATION OF 3D VELOCITY STRUCTURE IN THE SAN FRANCISCO BAY AREA
PHASE II: COLLABORATIVE RESEARCH WITH THE UNIVERSITY OF
CALIFORNIA, BERKELEY, AND THE UNIVERSITY OF MINNESOTA, DULUTH**

Douglas Dreger

Seismological Laboratory, University of California, Berkeley
215 McCone Hall #4760, Berkeley, CA 94720

Tel.: (510) 643-1719, FAX: (510) 643-5811, Email: dreger@seismo.berkeley.edu

David Dolenc

Large Lakes Observatory, University of Minnesota, Duluth
2205 E 5th Street, Duluth, MN 55812

Tel.: (218) 726-8136, FAX: (218) 726-6979, Email: ddolenc@d.umn.edu

Abstract

We have developed inversion of the teleseismic data to refine the 3D velocity model within the Santa Clara Valley (SCV) basins. The observation equation is first linearized and then solved iteratively by singular value decomposition. Synthetic waveforms as well as sensitivity functions are needed to obtain the solution. We use the elastic finite-difference code E3D (Larsen and Schultz, 1995) to calculate the waveforms and obtain the sensitivity functions numerically, by taking the difference of waveforms from perturbed and unperturbed models. The results showed that the method is stable and can be used to improve the velocity structure within the basin. Results suggested that slower velocity structure in the SCV basins than presently included in the USGS SF06 v8.3 velocity model could better explain the teleseismic observations. Results further showed that the method is not sensitive to the deeper parts of the basins (from 4 km to 5.75 km) as defined in the USGS SF06 v8.3 model. Inversion results with the SCV basins that extend only to 4 km depth provided similar results to the ones obtained with the deeper basins.

Project Results

We report on our development of the inversion of the teleseismic data to refine the 3D velocity model within the Santa Clara Valley (SCV) basins. Results from our previous work (Dolenc et al., 2005; Dolenc and Dreger, 2005) showed that teleseismic, local earthquake, and microseism data are all sensitive to the SCV basin structure. This suggested that they could be used to further improve the 3D velocity model. We developed inversion of the teleseismic observations to refine the USGS SF06 3D model velocity structure within the SCV basins. To reduce the extremely large model space, we invert for the velocity structure within the basins while the basin geometry, as defined in the USGS SF06 v8.3 velocity model, is held fixed. Basin geometry in the USGS model was mainly constrained by the inversion of the gravity data (Jachens et al., 1997; Brocher et al., 1997) and is one of the better known parameters in the model (R. Jachens, personal communication, 2005). Results from more recent reflection and refraction studies (Catchings et al., 2005; Catchings et al., 2006) confirmed the general basins geometry along their profiles.

We use the 3D elastic finite-difference code E3D (Larsen and Schultz, 1995) to simulate the teleseismic wavefields for the models with increasing levels of complexity in the basins. We prepared scripts that identify the SCV basins in the USGS model following the velocity contrast at the bottom of the basins. Once we have the SCV basins singled out from the rest of the model, we can assign them different properties. We prepared numerous variations of the model within the SCV basin that had

- laterally uniform velocity with a single velocity gradient,
- two to four vertical regions, each with its own velocity gradient.

Because of the computational limitations, the slowest velocities in the model were increased to a minimum S-wave velocity of 1 km/s. The slowest P-wave velocity was 1.75 km/s. The modeling was performed using 250-m grid spacing. Some of the modeling was also done using the finer 125-m grid spacing to evaluate the importance of including slower velocities. The size of the model used for modeling the teleseismic events was 125.25x145.25x42 km (see Fig. 1). To model the plane wave from the teleseismic events, we used a disc of point sources in the deepest homogeneous layer of the model, representing the upper mantle. In the next step we use the simulated wavefields to do the inversion following the approach developed by Aoi (2002). In his study, Aoi (2002) used the inversion scheme to estimate the 3D basin shape from the long-period strong ground motions. In this work we keep the basin geometry fixed and invert for the velocity structure within the basins.

Formulation of the inversion

To obtain the model that best describes the data, the observation equation

$$u_i(x_m, t_n; \bar{p}) \cong \tilde{u}_{imm} \quad (1)$$

needs to be solved. The $u_i(x_m, t_n; \bar{p})$ is the i-th component of the synthetic waveform for the model parameter vector \bar{p} and \tilde{u}_{imm} is the i-th component of the data observed at x_m at the n-th time step t_n . The equation is nonlinear with regard to the model parameter \bar{p} and in order to solve it iteratively, the left side is first expanded in Taylor series about the parameter \bar{p}^0 (initial model). It is then linearized by omitting the higher-order terms. Resulting linearized observation equation for the l-th iteration can then be written as

$$u_i(x_m, t_n; \bar{p}^l) + \sum_{k=1}^K \left. \frac{\partial u_i}{\partial p_k} \right|_{\bar{p}=\bar{p}^l} \partial p^k \cong \tilde{u}_{imm} \quad (2)$$

where \bar{p}^l is the model parameter estimated in the (l-1)-th iteration. To solve this non-square matrix equation, we need to obtain the sensitivity functions $\frac{\partial u_i}{\partial p_k}$. They can be calculated numerically by using the finite-difference approximation by first modeling the waveforms for the perturbed and unperturbed models and then calculating the difference of the waveforms

$$\left. \frac{\partial u_i}{\partial p_k} \right|_{\bar{p}=\bar{p}'} \equiv \frac{u_i(x_m, t_n; \bar{p}' + \Delta \bar{p}'_k) - u_i(x_m, t_n; \bar{p}')}{\Delta p_k} \quad (3)$$

where $\Delta \bar{p}'_k = (0, 0, \dots, \Delta p_k, \dots, 0)$. The equation (2) now represents a set of simultaneous linear equations whose coefficient matrix is nonsquare and singular value decomposition method (SVD; Press, 1999) can be used to solve it. The model parameters are iteratively modified by linear iteration method until the residual

$$\sqrt{\sum_{i,m,n} (\tilde{u}_{imm} - u_i(x_m, t_n; \bar{p}'))^2} \quad (4)$$

is sufficiently small and the model has converged (Aoi, 2002).

Results

In our previous work we have used the synthetic data to test the stability of the inversion method. Although in these tests the previous version of the USGS 3D seismic velocity model (ver. 2) was used, the results showed that the original model could be retrieved (Dolenc et al., 2007). In the test inversions we used synthetic waveforms obtained with a selected target model instead of true observations. This was to test the inversion method while the target 3D velocity structure was known and based on the USGS ver. 2 velocity model.

In this work we used the USGS SF06 v8.3 3D velocity model and only changed the properties within the SCV basins (see Fig. 2). We modeled the $M_w 6.4$ teleseismic event that occurred near the coast of central Chile (07/29/1998, lat -32.30, lon -71.67, 58 km depth). The event was well recorded on the SCV seismic array stations and was also included in our previous modeling (Dolenc et al., 2005). The teleseism was modeled using the elastic finite-difference code E3D (Larsen and Schultz, 1995) as described in Dolenc et al. (2005).

To reduce the large modeling space, here we only inverted for the P-wave velocity in the SCV basins and used the empirical relationships from Brocher (2005)

$$v_s = 0.7858 - 1.2344v_p + 0.7949v_p^2 - 0.1238v_p^3 + 0.0064v_p^4 \quad (5)$$

$$\rho = 1.6612v_p - 0.4721v_p^2 + 0.0671v_p^3 - 0.0043v_p^4 + 0.000106v_p^5 \quad (6)$$

to set v_s and ρ . This allowed us to keep smaller number of independent parameters in the inversion (only P-wave velocity and its gradient for each layer) and thus significantly reduced the forward calculation computation time at each iteration step. This allowed us to test more models. Previous test that included synthetic data (Dolenc et al., 2007) showed that S-wave velocity could be used as an independent parameter in the inversion. On the other hand, previous test also showed that the method was not sensitive to reasonable changes in density.

The computations were performed on the BSL Linux cluster. The computation time for a single forward simulation that produced 60 s long waveforms was ~ 70 minutes when 16 cluster nodes and 2 processors per node were used. Each forward computation required ~ 4.5 GB of memory. To obtain the sensitivity functions (see equation 3), waveforms for the perturbed and unperturbed model had to be forward modeled at every iteration step. Since two parameters were

used for each layer, waveforms were computed at every iteration step for each model parameter variation. In addition, waveforms for the model obtained in the previous iteration (or the starting model for the first iteration) were also computed. The combined time for every iteration step was therefore about 500 minutes.

Although we have tested numerous model variations in the SCV basins as the starting models in the inversion, they all resulted in similar final models. Therefore we present here only two representative examples in more detail.

The first model included a single velocity layer in the SCV. It included a velocity gradient and the basins extended all the way to 5.75 km as defined in the USGS SF06 v8.3 velocity model. The model is shown and described in Fig. 4 and Table 1 and the results are presented in Figures 5-8.

The second example included the SCV basins that extended only to 4 km depth. The SCV basins in the USGS SF06 v8.3 model below 4 km were filled with the surrounding bedrock properties from the USGS SF06 model. The reason for this type of the model was (1) our preliminary results from work done here showed that when deeper part of the basin is used as a separate layer in the inversion, the layer properties are poorly constrained by the inversion, and (2) our initial analysis of the teleseismic events in the SCV (Dolenc et al., 2005) showed that teleseisms are not sensitive to basin structure deeper than ~4 km. This model is shown in Fig. 9 and Table 2 and the results are presented in Figures 10 and 11.

Discussion

The results showed that the inversion method is stable and can be used to improve the velocity structure within the SCV basins. Results from inversion with different starting models consistently suggested that slower velocity structure in the SCV basins than presently included in the USGS SF06 v8.3 velocity model could better explain the teleseismic observations. Results further showed that the method is not sensitive to the deeper parts of the basins (from 4 km to 5.75 km) as defined in the USGS SF06 v8.3 model and that inversion results with SCV basins that extend only to 4 km depth provided similar results to the ones obtained with the deeper basins. The waveforms presented in Figures 7 and 8 show that a slower model in the SCV basins than the USGS SF06 v8.3 can improve how well we can fit the observations. The results also showed that more work is needed and that higher resolution modeling that would allow inclusion of slower velocities should be included to better model the P-wave coda.

Conclusions

Velocity structure in the SCV basins can be improved by the inversion of the teleseismic data. Since the finite-difference code is used to calculate the sensitivity functions at each iteration step, this method can become computationally expensive, particularly if the model includes many free parameters and the number of iterations needed to reach the final model is not small.

Results suggested that slower velocity structure in the SCV basins than presently included in the USGS SF06 v8.3 velocity model could better explain the teleseismic observations. Results further showed that the method is not sensitive to the deeper parts of the basins (from 4 km to 5.75 km) as defined in the USGS SF06 v8.3 model and that inversion results with SCV basins that extend only to 4 km depth provide similar results to the ones obtained with the deeper basins.

Results also suggest that further work is needed to better understand the teleseismic waveforms observed in the SCV. Future work should attempt to model basin shape in addition to the velocity structure in the basins by including parameters describing basin shape as free

parameters in the inversion. Also, finer grid simulations that would permit modeling of slower velocities would provide better modeling of the P-wave coda.

References

Aoi, S., 2002, Boundary shape waveform inversion for estimating the depth of three-dimensional basin structures: *Bulletin of the Seismological Society of America*, v. 92, p. 2410-2418.

Brocher, T. M., 2005, Empirical relations between elastic wavespeeds and density in the Earth's crust, *Bulletin of the Seismological Society of America*, v. 95, p. 2081-2092.

Brocher, T., B. Aagaard, R. Simpson, and R. Jachens, 2006, The new USGS 3D seismic velocity model for northern California: *Seismological Research Letters*, v. 77, p. 271.

Brocher, T. E., E. E. Brabb, R. D. Catchings, G. S. Fuis, T. E. Fumal, R. C. Jachens, A. S. Jayko, R. E. Kayen, R. J. McLaughlin, T. Parsons, M. J. Rymer, R. G. Stanley, and C. M. Wentworth, 1997, A crustal-scale 3-D seismic velocity model for the San Francisco Bay area, California: *EOS Trans. AGU.*, v. 78, F435.

Catchings, R. D., G. Gandhok, M. R. Goldman, C. E. Steedman, and R. Hanson, 2005, Near-surface structure and velocities of the northeastern Santa Cruz Mountains and the western Santa Clara Valley, California from seismic imaging: U.S. Geological Survey Open-File Report, (in press).

Catchings, R. D., M. R. Goldman, and G. Gandhok, 2006, Structure and velocities of the northeastern Santa Cruz Mountains and the western Santa Clara Valley, California, from the SCSI-LR seismic survey: U.S. Geological Survey Open-File Report 2006-1014.

Dolenc, D. and D. Dreger, 2005, Microseisms observations in the Santa Clara Valley, California: *Bulletin of the Seismological Society of America*, v. 95, p. 1137-1149.

Dolenc, D., D. Dreger, and S. Larsen, 2005, Basin structure influences on the propagation of teleseismic waves in the Santa Clara Valley, California: *Bulletin of the Seismological Society of America*, v. 95, p. 1120-1136.

Dolenc, D., D. Dreger, and S. Larsen (2007). Simultaneous inversion of the teleseismic, local, and microseisms observation for the velocity structure within the Santa Clara Valley basins, *Seism. Res. Lett.*, 78, 310.

Jachens, R. C., R. F. Sikora, E. E. Brabb, C. M. Wentworth, T. M. Brocher, M. S. Marlow, and C. W. Roberts, 1997, The basement interface: San Francisco Bay area, California, 3-D seismic velocity model: *EOS Trans. AGU.*, v. 78, F436.

Larsen, S. and C. A. Schultz, 1995, ELAS3D: 2D/3D elastic finite-difference wave propagation code: Technical Report No. UCRL-MA-121792, p. 1-19.

Press, W. H., 1999, FORTRAN numerical recipes: Cambridge England, New York, NY,
Cambridge University Press.

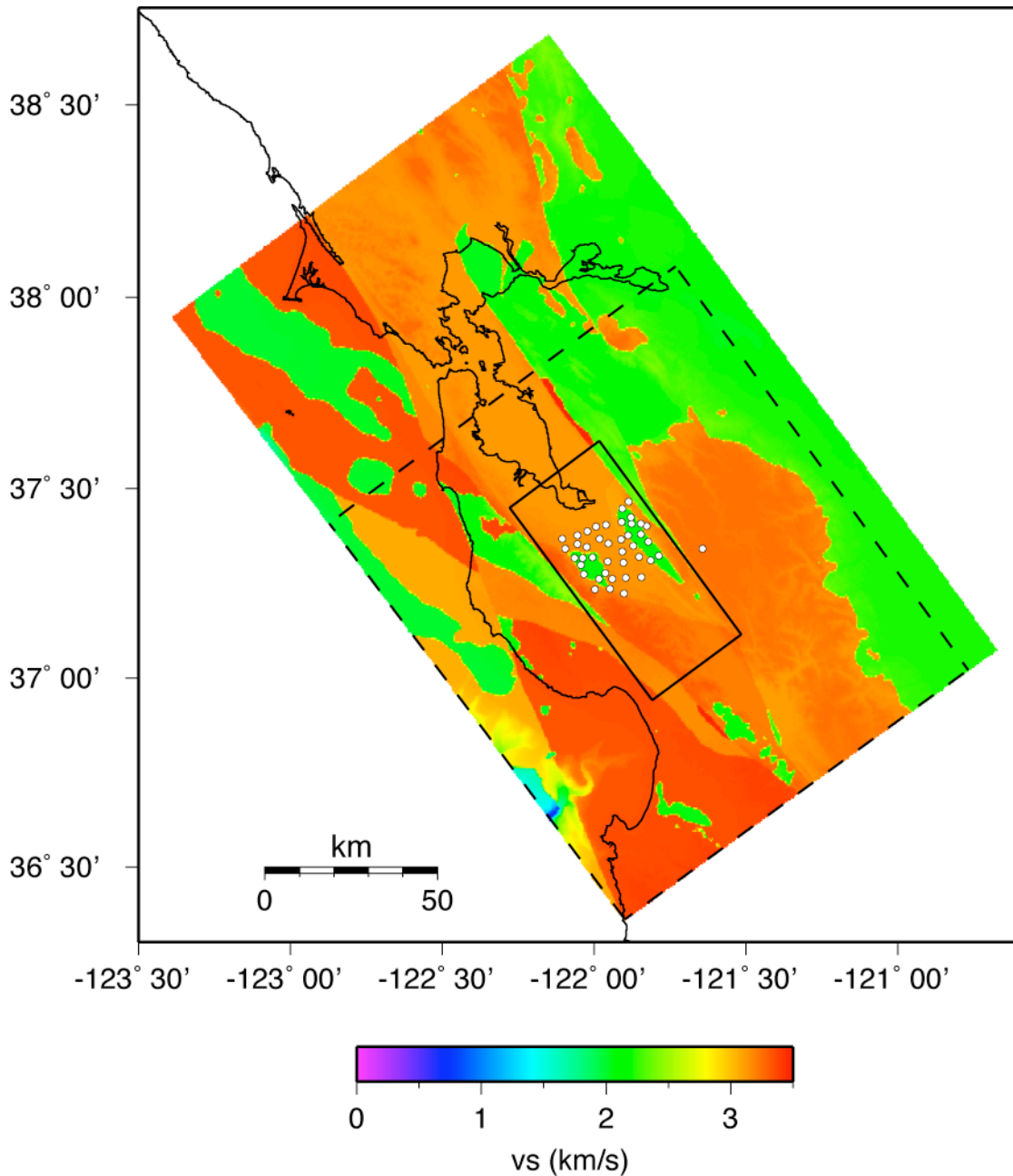


Figure 1. Location of the temporary SCV seismic array south of the San Francisco Bay (circles). As an example of 3D velocity model, a 2500 m depth section (v_s) from the USGS SF06 v8.3 3D velocity model of the Bay Area is shown. The dashed box shows the size of the model used in the E3D finite-difference simulations. The solid box shows the SCV region. Within this region SCV basins were identified and their properties changed for the use in the inversion (see Fig. 2).

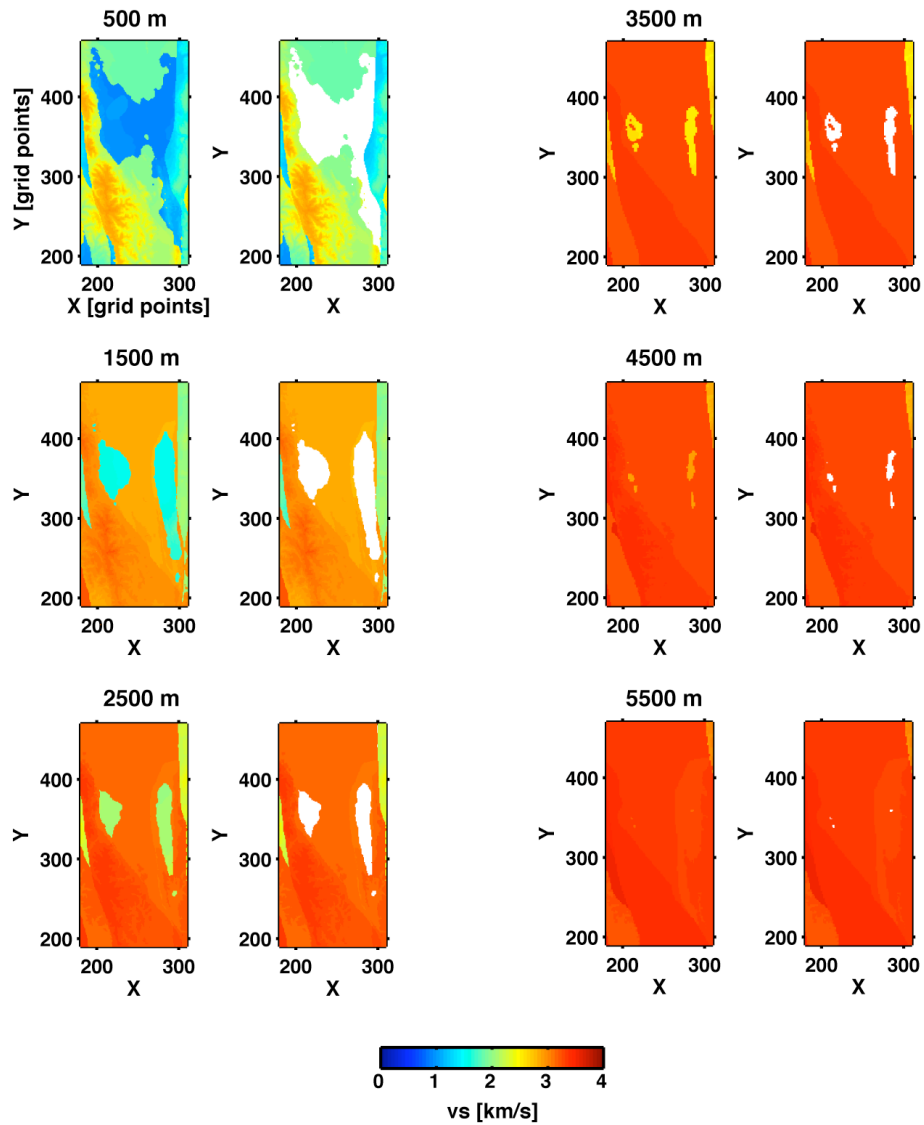


Figure 2. V_s in the SCV region (see solid box in Fig. 1) from the USGS SF06 v8.3 3D velocity model. To the right of each depth section is shown a result of the SCV basins identification. The regions that we identified as the SCV basins are shown as white. These regions were later filled with different properties to be used in the inversion. Grid points of the 250 m grid are shown on the x- and y-axes.

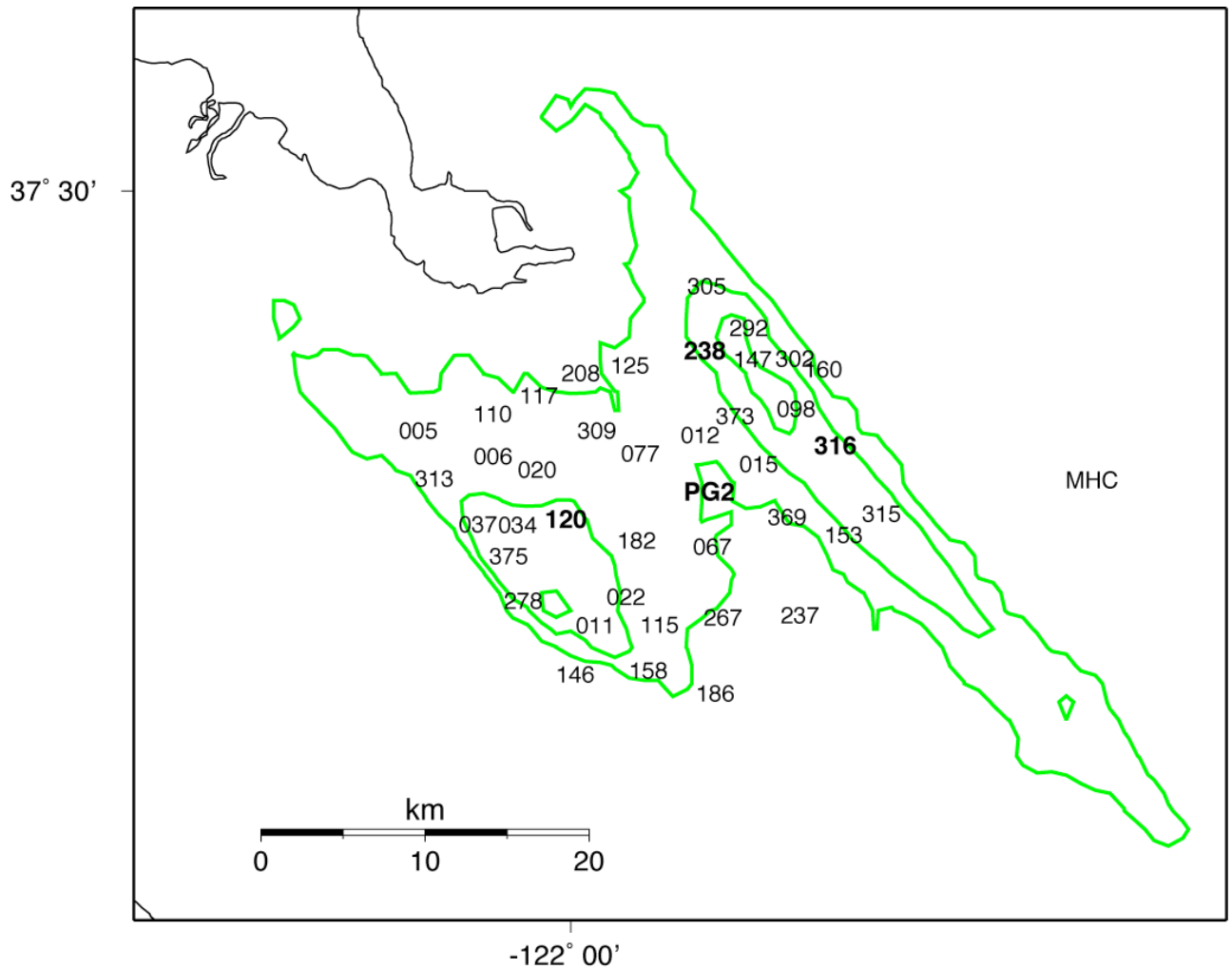


Figure 3. Closer look at the SCV region. Numbers indicate SCVSE seismic stations. Green lines denote the contours of the basins from the USGS SF06 v8.3 3D velocity model at 500 m, 2500 m, and 4500 m depth. Station MHC is the permanent station of the Berkeley Digital Seismic Network. Stations in bold (120 over the Cupertino basin, 238 and 316 over the Evergreen basin, and PG2 between the two basins) are shown in Figures 5, 6, 10, and 11. Results for all stations are shown in Figures 7 and 8.

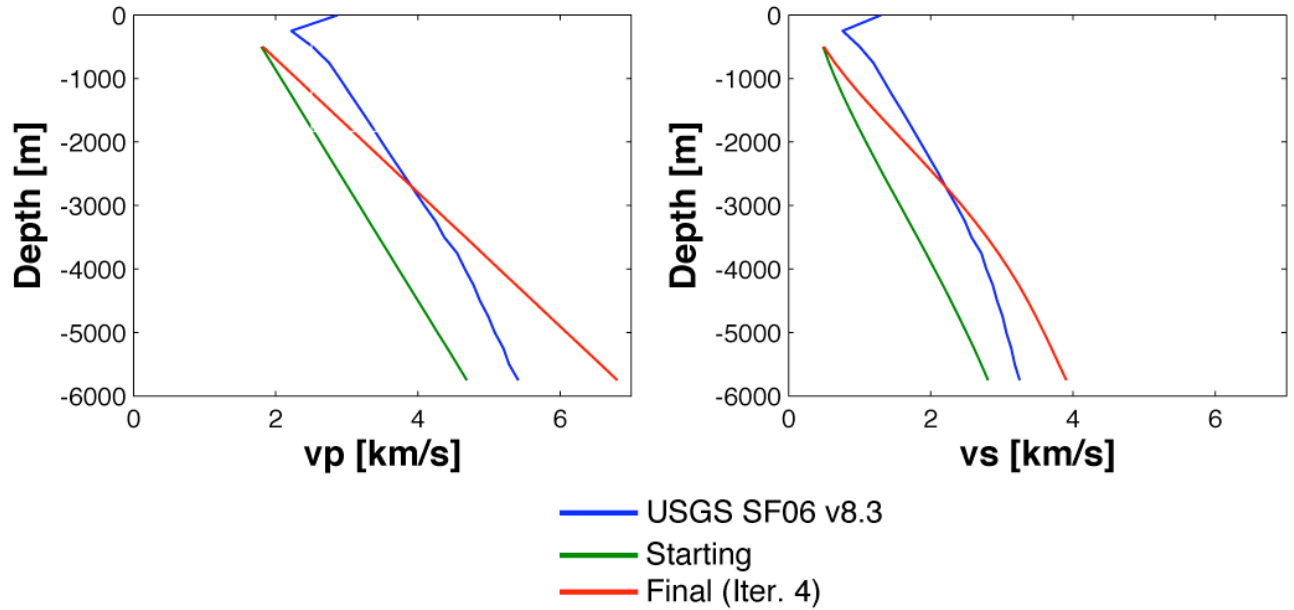


Figure 4. Velocities in the SCV basins for the USGS SF06 v8.3 model, the initial, and final model. Single velocity layer with gradient is used for the entire SCV basins. Deepest parts of the basins extend to 5.75 km as defined in USGS SF06 v8.3 model.

Table 1.

P-wave velocity in the SCV basins at 500 m depth for the USGS SF06 v8.3 model, starting, and final model after four iterations. Also listed is v_p gradient with depth (below 500 m depth). The model included a single velocity layer with gradient. The basins extend to 5.75 km as defined in USGS SF06 v8.3 model (see Fig. 4).

Parameter	USGS SF06 v8.3	Starting model	Final model (Iter. 4)
v_p [km/s]	2.52	1.8	1.82
$\partial v_p / \partial z$ [km/s / km]	0.55	0.55	0.95

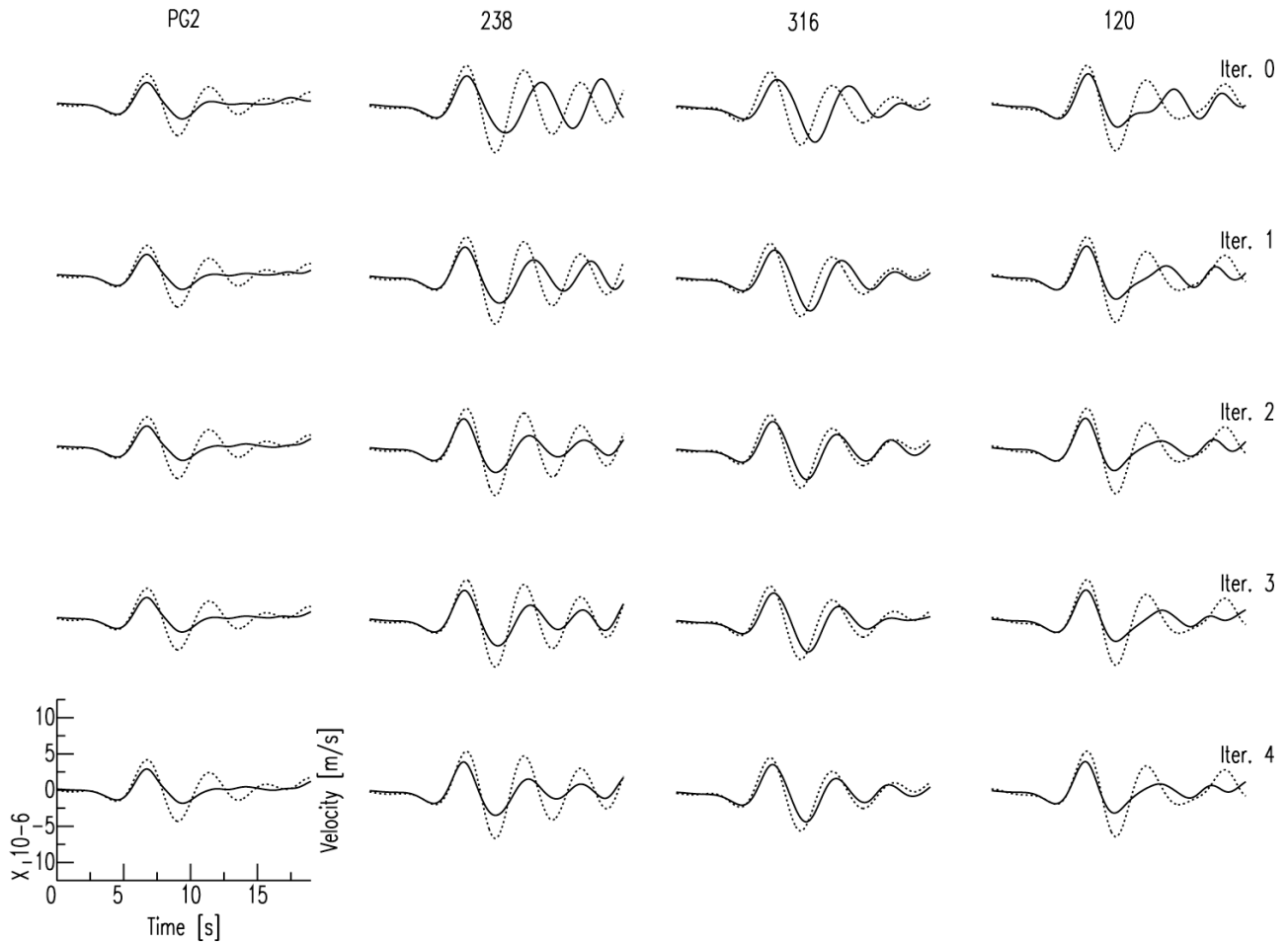


Figure 5. Inversion result for the case of the SCV basins filled with a single velocity layer with gradient. Waveforms for four SCV stations (38 used in the inversion) are shown for the initial model (solid, top row) and for a model as it was after iterations 1-4 (solid, bottom rows). Observed waveforms are shown for comparison (dotted). Shown are first 20 s of the waveforms as only this time window was used in the inversion. Velocities in the SCV basins for the initial and final model are shown in Fig. 4. Waveforms for the initial and final model for all stations are shown in Figure 7.

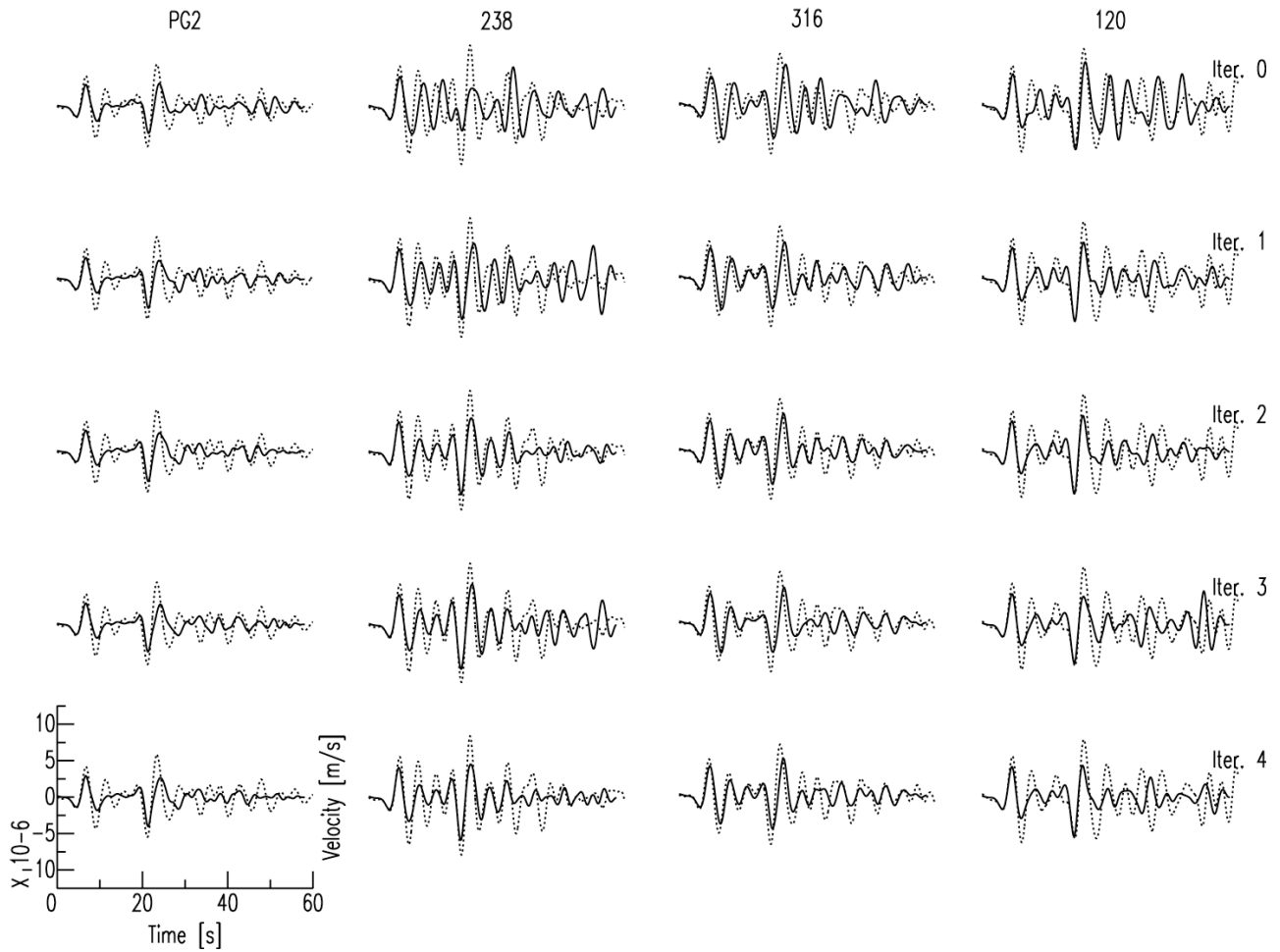


Figure 6. Same as Fig. 5, only that 60 s time windows are now shown. In addition to P-wave, pP-wave can be seen arriving just after the first 20 s. Waveforms for the first 20 s were used in the inversion. The plots show how the model changes affect the P-wave coda following the pP arrival.

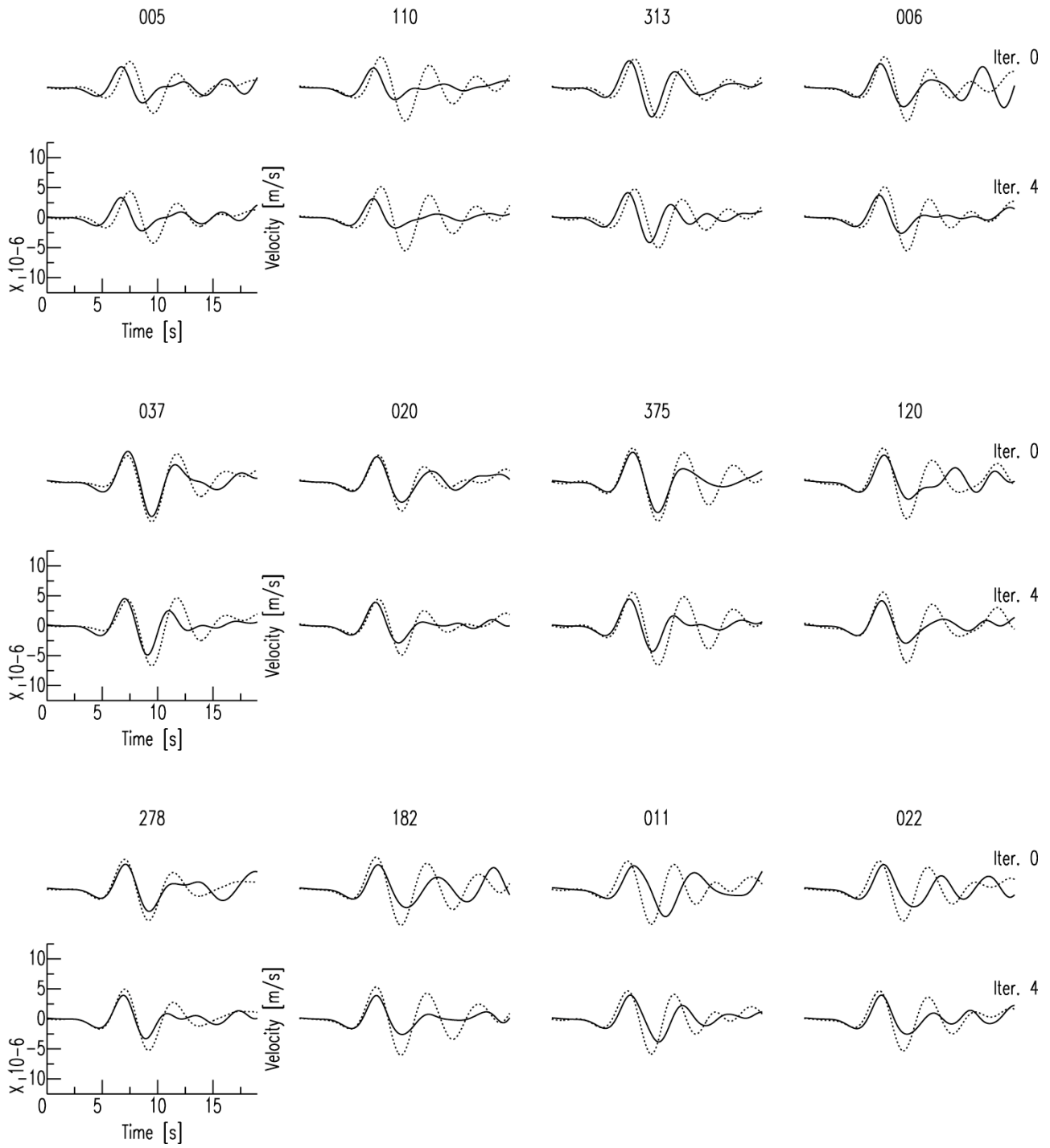


Figure 7. Same as Fig. 5, only that now only waveforms for the initial and final model are shown. Waveforms for all stations that were used in the inversion are plotted. Figure continued on next pages. See Fig. 3 for stations locations.

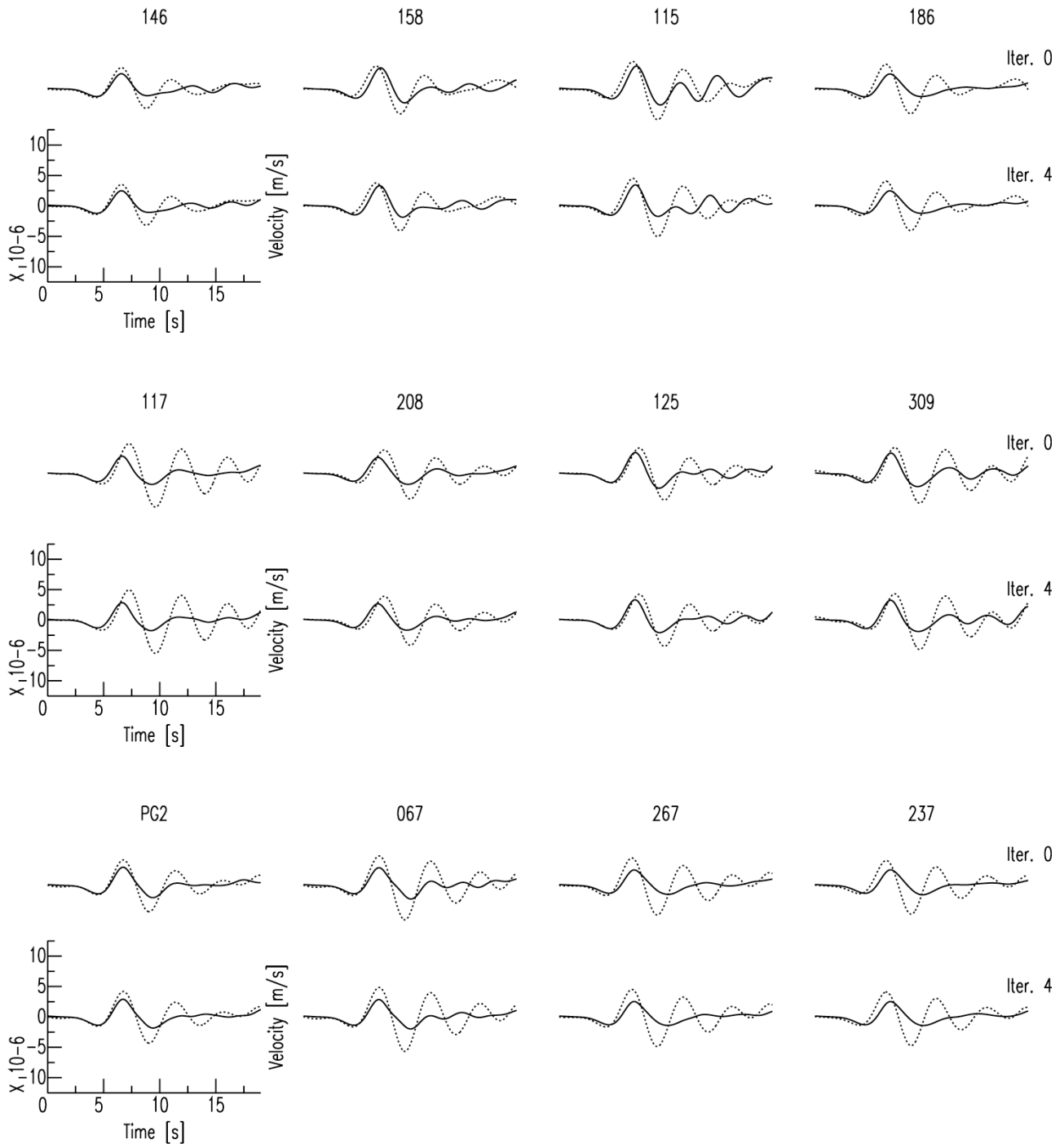


Figure 7. Continued.

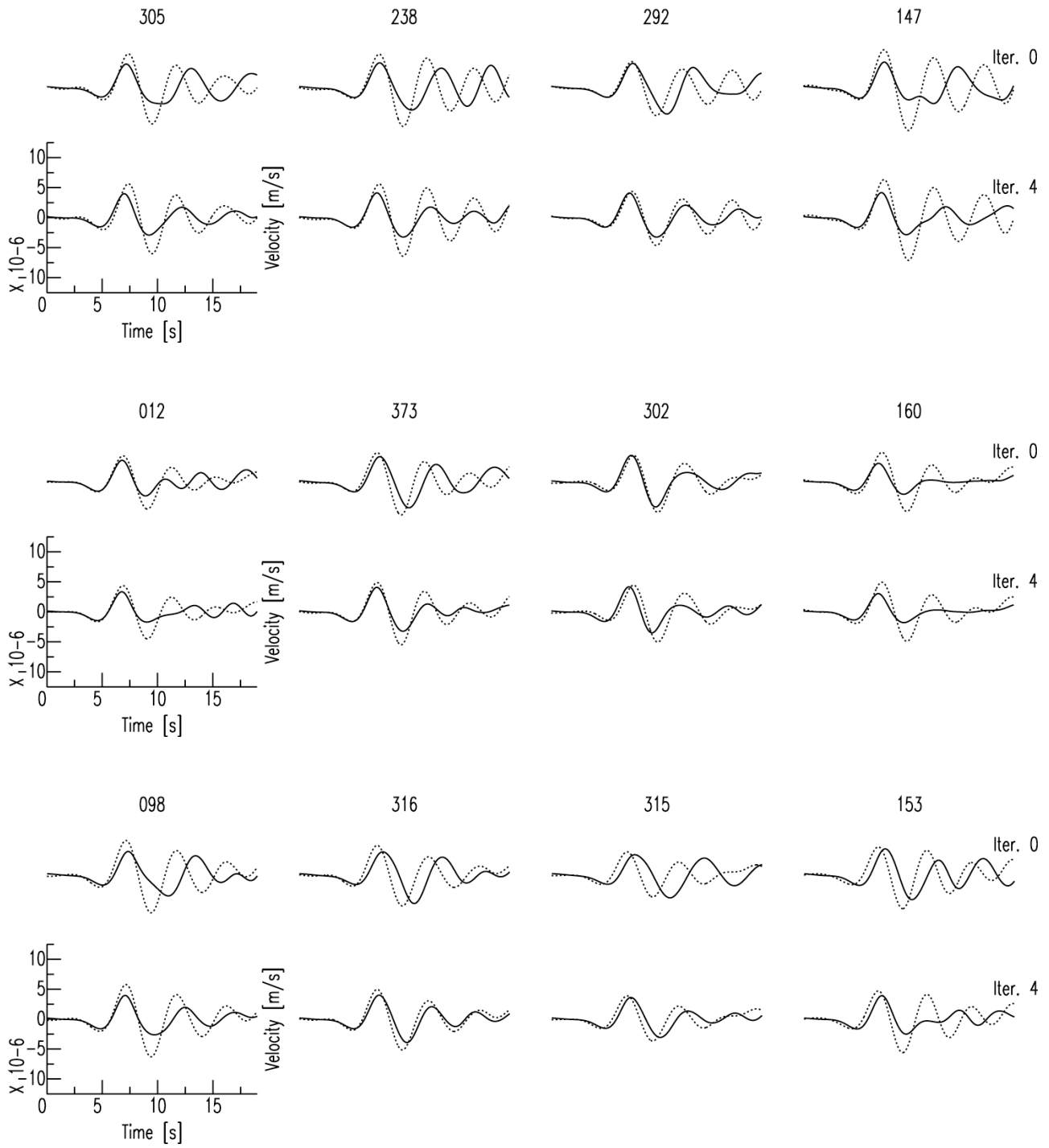


Figure 7. Continued.

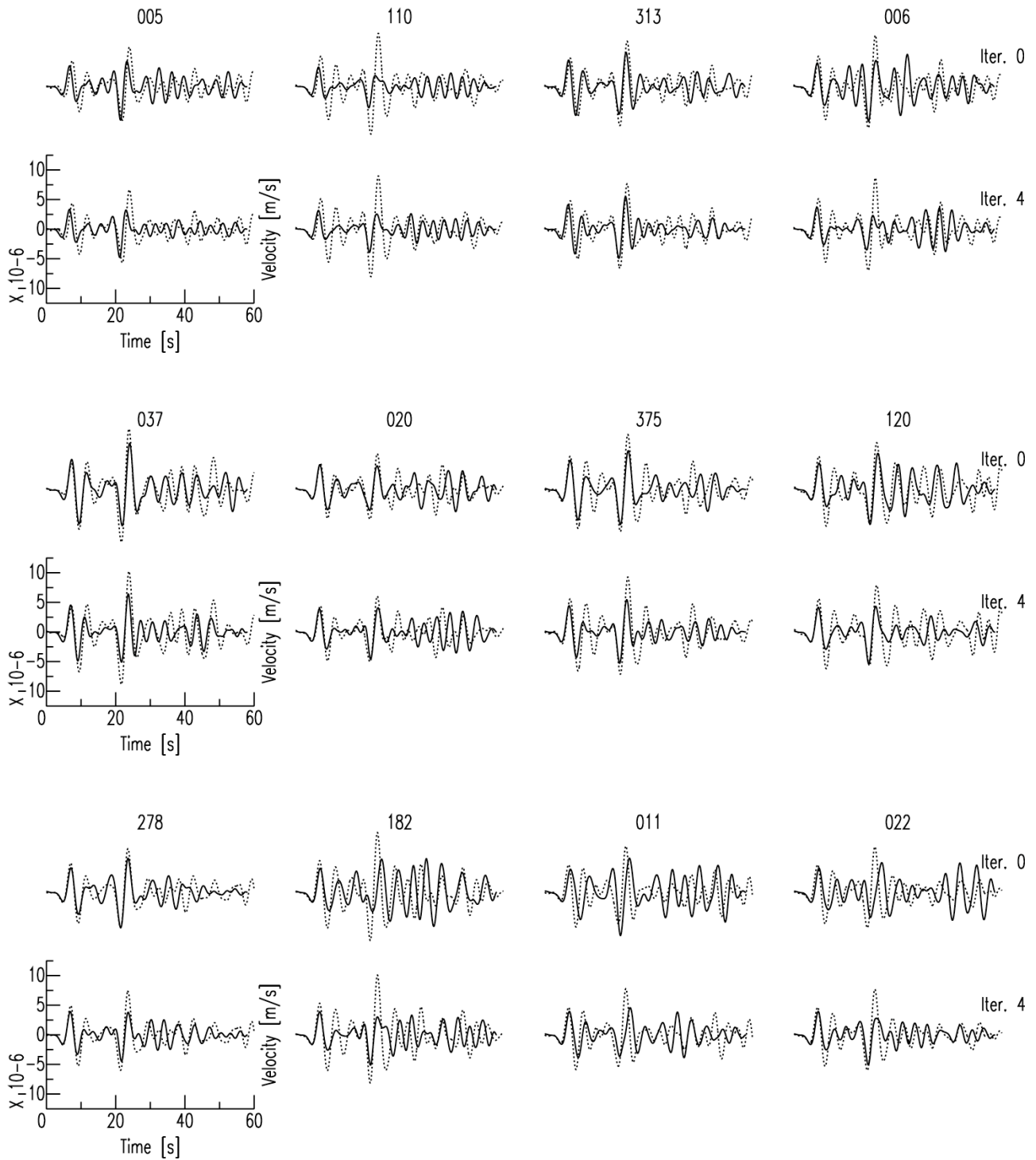


Figure 8. Same as Fig. 6, only that now only waveforms for the initial and final model are shown. Waveforms for all stations that were used in the inversion are plotted. Figure continued on next pages. See Fig. 3 for stations locations.

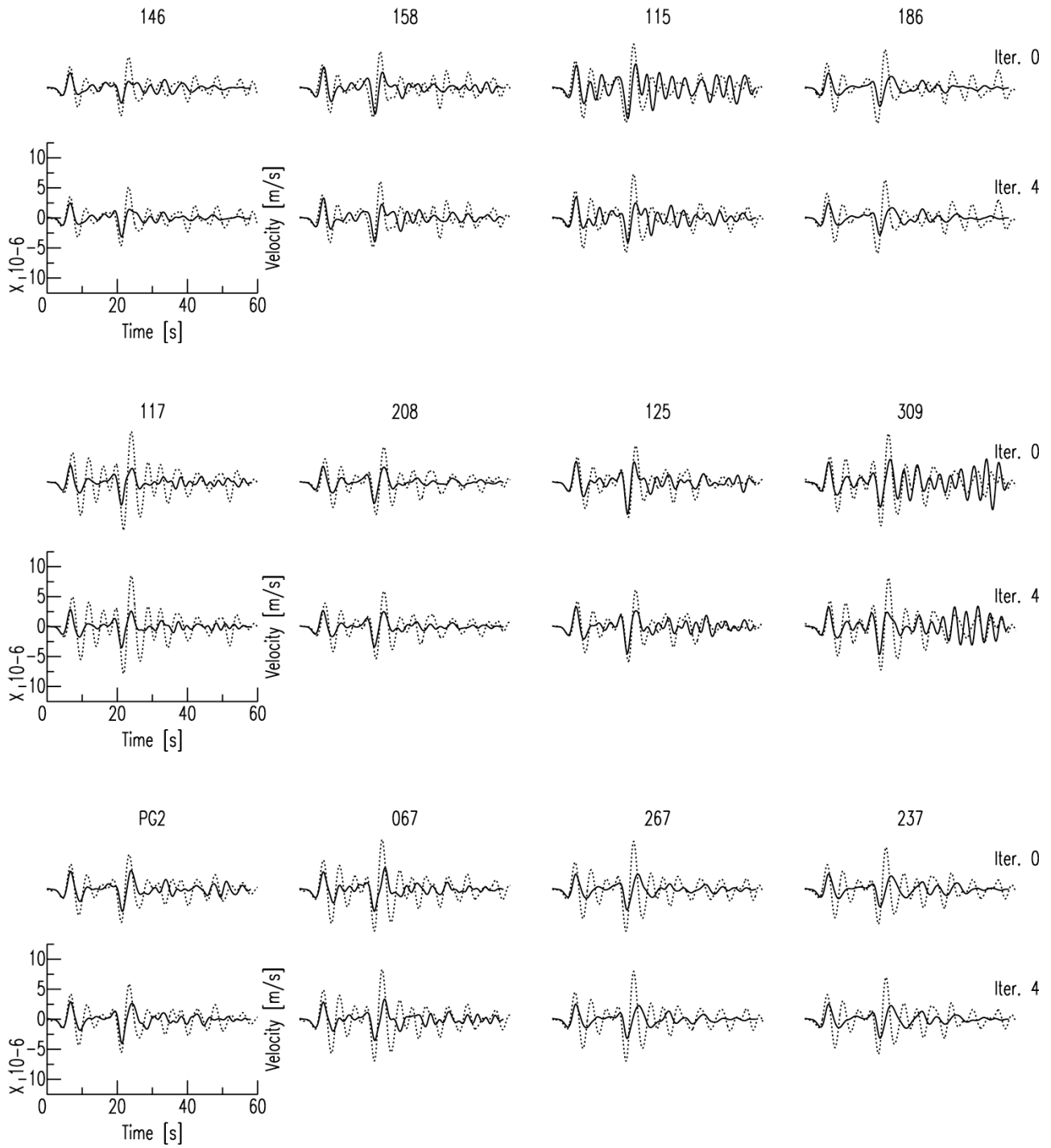


Figure 8. Continued.

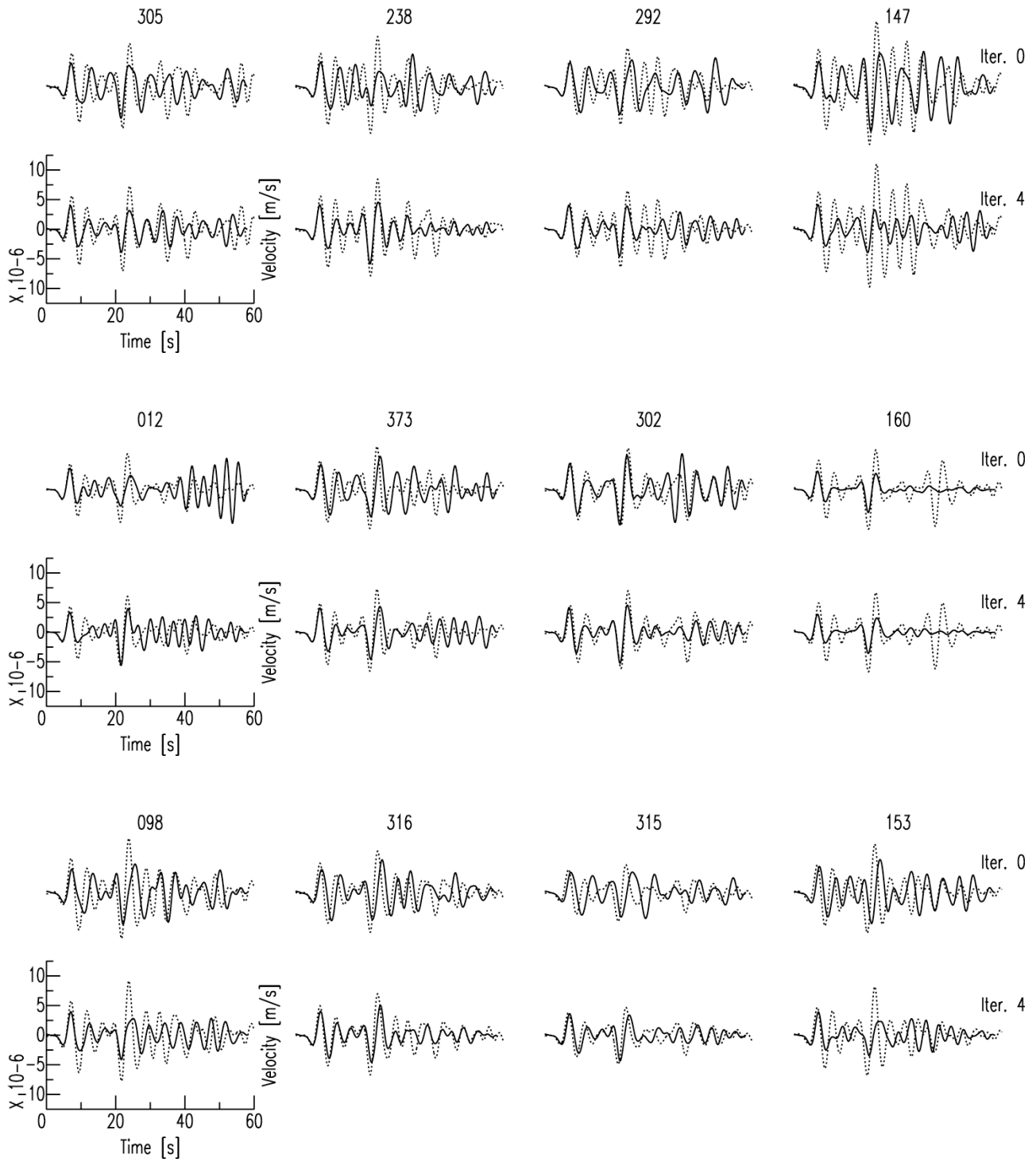


Figure 8. Continued.

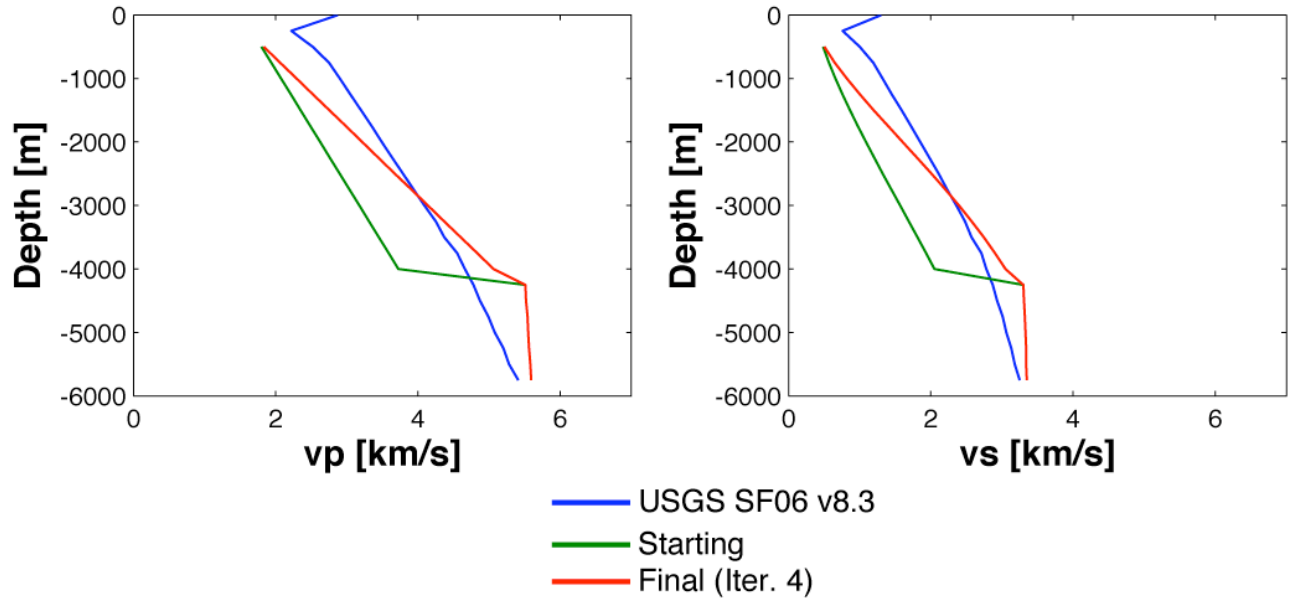


Figure 9. Velocities in the SCV basins for the USGS SF06 v8.3 model, the initial, and final model. Single velocity layer with gradient is used for the SCV basins down to 4 km depth. Basins below 4 km depth are filled with surrounding bedrock properties as defined in the USGS SF06 v8.3 model.

Table 2.

P-wave velocity in the SCV basins at 500 m depth for the USGS SF06 v8.3 model, starting, and final model after four iterations. Also listed is v_p gradient with depth (below 500 m depth). The model included a single velocity layer with gradient, however, unlike in the USGS SF06 v8.3 model, the basins extended only to 4 km depth. Basins below 4 km depth were filled with surrounding bedrock properties.

Parameter	USGS SF06 v8.3	Starting model	Final model (Iter. 4)
v_p [km/s]	2.52	1.8	1.83
$\partial v_p / \partial z$ [km/s / km]	0.55	0.55	0.92

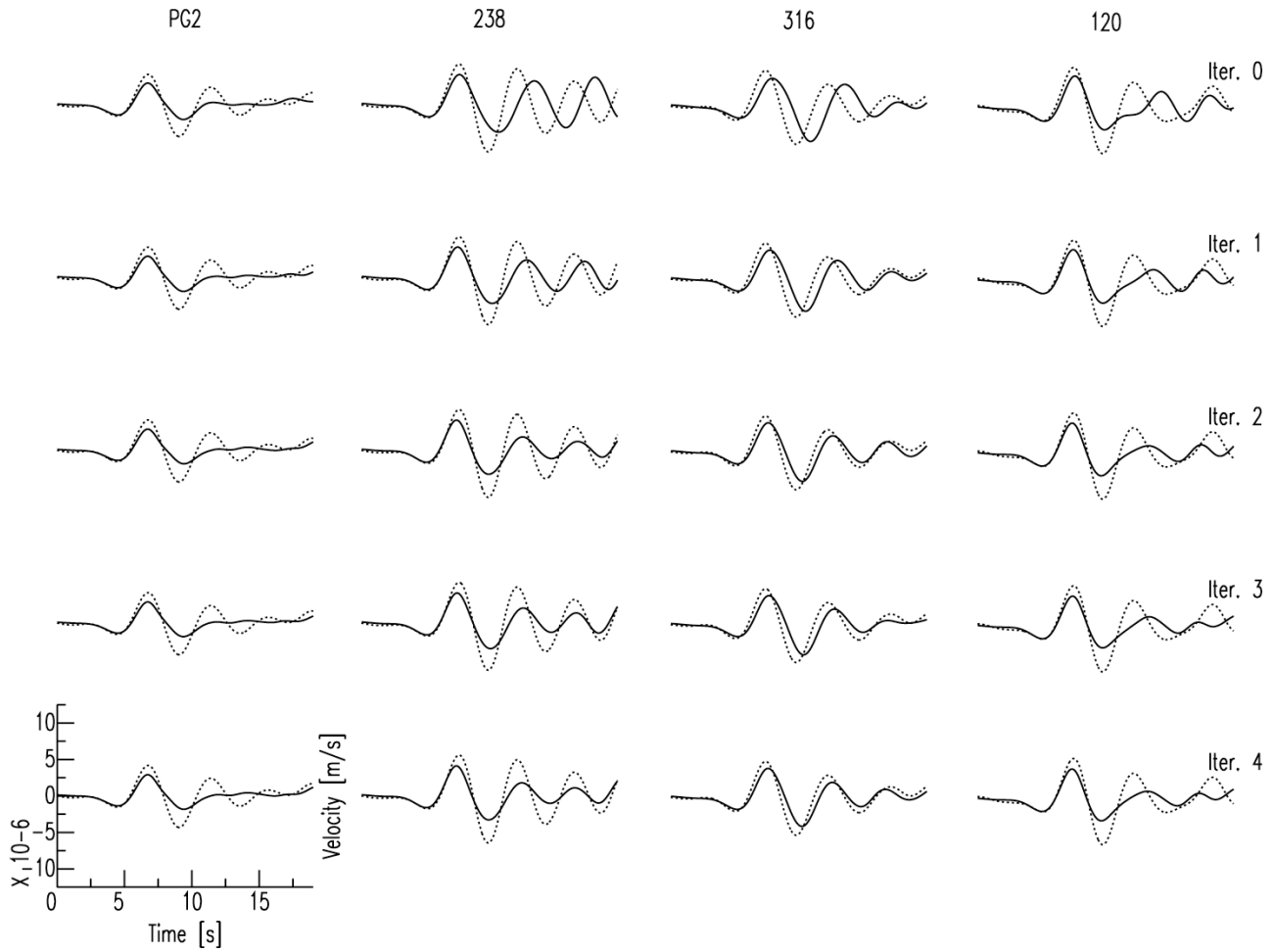


Figure 10. Inversion result for the case of the SCV basins filled with a single velocity layer (with gradient) that extends to 4 km depth. Basins below 4 km depth were filled with surrounding bedrock properties as defined in the USGS SF06 v8.3 model. Waveforms for four SCV stations (38 used in the inversion) are shown for the initial model (solid, top row) and for a model as it was after iterations 1-4 (solid, bottom rows). Observed waveforms are shown for comparison (dotted). The four stations are representative of the Cupertino basin (120), Evergreen basin (238 and 316), and the region between the two basins (PG2; see Fig. 3). Shown are first 20 s of the waveforms as only this time window was used in the inversion. Velocities in the SCV basins for the initial and final model are shown in Fig. 9.

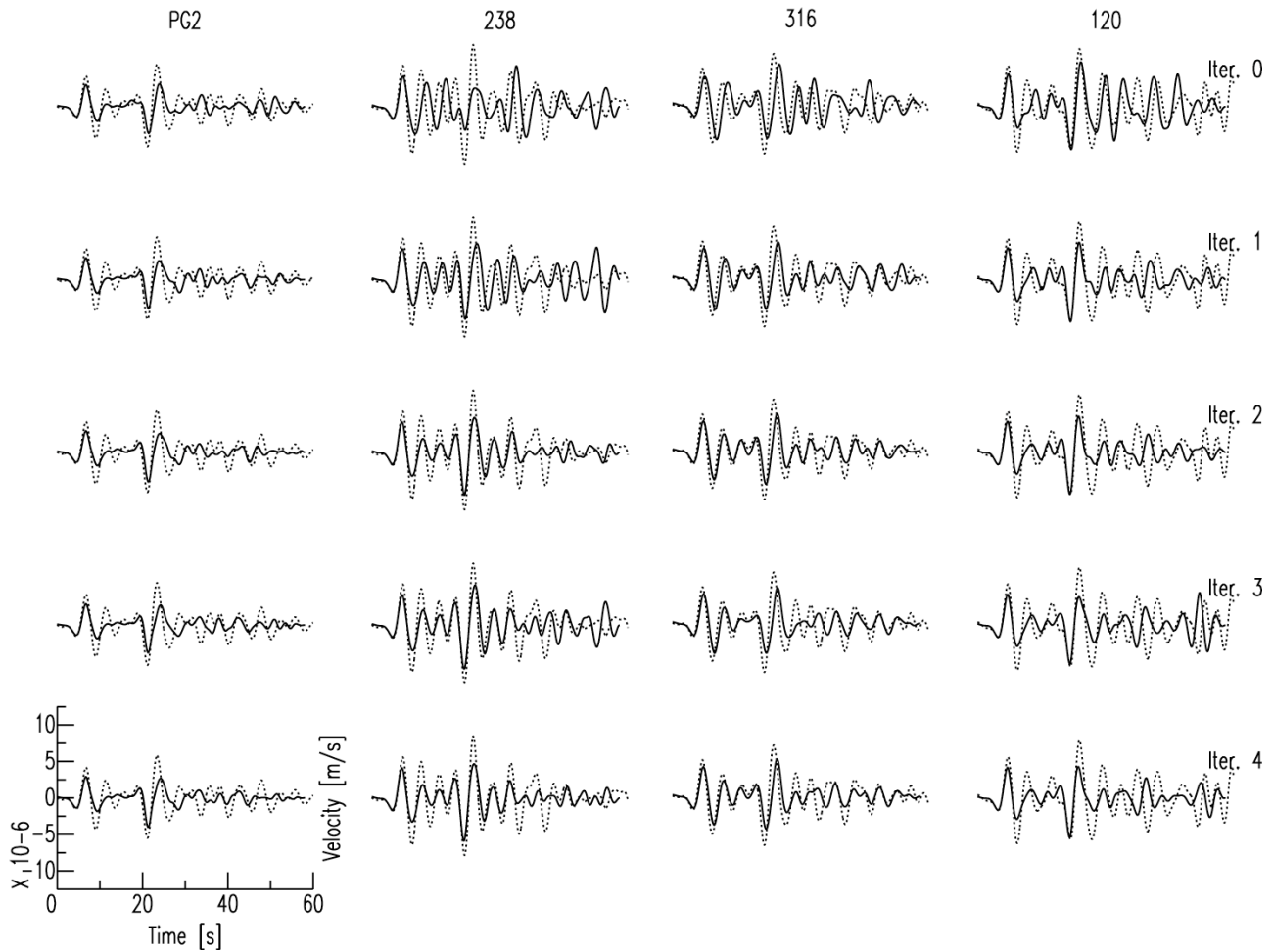


Figure 11. Same as Fig. 10, only that 60 s time windows are now shown. In addition to P-wave, pP-wave can be seen arriving just after the first 20 s. Waveforms for the first 20 s were used in the inversion. The plots show how the model changes affect the P-wave coda following the pP arrival.

Peer-Reviewed Reporting of Results

Dolenc and Dreger are preparing a manuscript for submission to Bulletin of the Seismological Society of America. It describes results of the inversion presented in this report.